MDPI

Article

Evaluation of the Mechanical Properties of Lightweight Foamed Concrete at Varying Elevated Temperatures

Md Azree Othuman Mydin

School of Housing, Building and Planning, Universiti Sains Malaysia, Penang 11800, Malaysia; azree@usm.my

Abstract: Lightweight foamed concrete (LFC) made from cementitious materials with air pores entrapped in the matrix by mechanically entrained foam in the mortar slurry has several economic and environmental benefits. Most recently, LFC has been heralded as the next generation of lightweight construction industry concrete because of its versatility and technological advancements. Owing to its many desirable qualities, including low density, low cost, low thermal conductivity, low dimensional change, amazing load-bearing capacity, great workability, and low weight, it is considered an adaptable and flexible construction material. Given that LFC is a brittle building material and since fire is among the most frequent catastrophes to affect structures, it is crucial to consider the structural performance of LFC subjected to high temperatures. Hence, this experiment attempts to ascertain the effect of varying elevated temperatures on the LFC's strength properties. Three LFC densities of 500, 1000 and 1500 kg/m^3 were prepared. The LFC specimens were exposed to predetermined ambient and elevated temperatures of 20, 100, 200, 300, 400, 500, 600, 700 and 800 °C, and the LFC samples were assessed for porosity, compressive and flexural strengths. The outcomes of this investigation showed that, regardless of density, the loss of LFC stiffness exposed to elevated temperatures happened primarily after 90 °C. This shows that the underlying process triggering stiffness loss is internal cracking, that transpires when water grows and dissolves from a porous medium. Lowering the LFC dry density diminishes its strength and rigidity. The LFC-normalized strength and stiffness–temperature relationships of various dry densities, on the other hand, are very comparable. From ambient temperature up until 400 °C, all densities exhibit a moderate and constant loss in strength and stiffness. Nevertheless, the decline is faster up to 600 °C or 800 °C, at which point it loses its ability to support any given weight. This study emphasized the necessity for more study and codes' provisions that take into consideration various LFC constituent types and cutting-edge construction material technologies.

Keywords: foamed concrete; strength; compression; bending; fire; elevated temperatures; stiffness; Young's modulus

1. Introduction

The majority of physical infrastructure consists of buildings, which are crucial to a nation's socioeconomic development. Many structures are made to last for many years and to offer residential and practical services to a large number of people throughout their design lives. Structures are susceptible to several natural and man-made dangers during this prolonged period, which may cause a complete or partial failure of the building and the incapacity to carry out building operations [1]. Such destruction or inability can put inhabitants' lives and safety in peril during a hazard, as well as cause significant direct and indirect financial losses. To ensure life and structural safety throughout their design life, structures are built to withstand several projected dangers. Fire is one such serious risk that can happen in buildings [2].

Concrete manufacturing needs a large number of natural resources [3]. A typical batch of concrete uses about 15% cement and 75% coarse particles by mass, according to sources [4]. Around 7% of the carbon dioxide (CO_2) that is emitted globally each year

is produced by the cement industry, which is harmful to the environment [5]. Natural aggregates are continuously extracted and used, which has a negative impact on the ecosystem and depletes the remaining resources. In addition, concrete mass production necessitates a substantial quantity of potable water, which is another major concern in the construction sector [6]. Therefore, it is essential to make concrete that has a minimal impact on the environment and reduces the consumption of natural sources [7,8].

The usage of concrete in high-temperature applications has increased recently. Concrete may suffer severe damage from the chemical and physical changes that are brought on by high temperatures, which can significantly reduce its mechanical properties and durability performance [9]. Concrete deteriorates due to severe physical and chemical changes caused by extreme heat. Even though concrete is thermally resistant to other building materials, it suffers catastrophic damage when exposed to fire and elevated temperatures. Concrete has numerous irretrievable natural and chemical alterations when heated to a high temperature. This may also cause the concrete member's structural integrity to deteriorate, resulting in spalling and ultimately the element's demise. The endurance of concrete structures is significantly impacted by the physical deterioration processes that are accelerated by high temperatures, which can lead to dangerous structural failures [10]. When cement-based material is exposed to high temperatures, the properties of the constituent materials used in its production have a significant impact on how well it performs. These attributes include the aggregates' density and void content as well as the cement paste and aggregate's thermal compatibility and adhesion [11]. Calcium silicate hydrate experiences significant changes when the temperature rises over 110 °C, together with the release of chemically bonded water and the dehydration process. The shrinkage of concrete is also influenced by calcium hydroxide dissociation, which occurs at temperatures higher than 530 °C. Microcracks in the concrete microstructure are a result of dehydration and the thermal expansion of particles at 300 °C [12]. The temperatures at which calcium hydroxide and calcium silicate hydrate disintegrate are 400 °C and 600 °C, respectively. Around 800 °C, the two hydration products begin to dissolve more quickly, significantly decreasing the strength of the concrete. Additionally, quicklime is created when calcium hydroxide breaks down [13]. Because calcium hydroxide can be reconstituted when calcium oxide comes into touch with water during the cooling phase, the reaction is reversible. These repeated reactions cause the concrete microstructure to expand and contract, which causes cracking [14].

Lightweight foamed concrete (LFC) is regarded as an advanced and adaptable generation of lightweight construction industry concrete. It is a flexible construction material due to its attractive characteristics, which include exceptional thermal-insulating capabilities, minimal dimensional variations, outstanding load-bearing capacity, and low density [15]. LFC comprises a minimum of 15% entrained foam in the cement mortar and has air pores trapped in the matrix using an appropriate surfactant [16]. By stirring the air with a foaming ingredient that has been diluted in water, the air pores are initiated. The foam is then gently combined with the cement slurry to create LFC [17]. When the stable foam is incorporated into the base mix of LFC, the resulting material has a lower self-weight, greater workability, and superior insulating qualities, but less strength than standard-strength concrete [18]. As a result, LFC can be manufactured in any area, regardless of their final form or the size of the construction in which it is housed [19].

Compared to conventional concrete, the manufacture of LFC is both energy- and water-efficient [20,21]. It is an inventive method that lessens the use of water, cement, and fine filler without creating environmental degradation by substituting a portion of the concrete with air bubbles [22,23]. To take advantage of LFC's lightweight and effective insulating qualities, there has been an increasing utilization of LFC as a semi-structural component in buildings in recent years [24,25]. It is important to note that many studies on LFC to date have only looked at its properties at room temperature. Among them, the majority regarded LFC's mechanical qualities with only a small impact on its thermal properties. There is a severe lack of hard data on the effectiveness of fire barriers. However, the information gained from

these studies provides a solid foundation for future studies of the mechanical properties of LFCs at room temperature. Using SEM analysis as well as stereomicroscopy, Lin et al. [26] analyzed the concrete microstructure that had been exposed to elevated temperatures. They determined that unhydrated OPC grains and calcium oxide may be rehydrated by absorbing moisture from the ambient medium and subsequently refilling the voids. C-H, $CaCO_3$, C-S-H, and non-evaporable water were studied by Schneider and Herbst [27] to determine their chemical reactions and behavior at different temperatures. They discovered that microcracks, changes in the material's internal structure, and crack openings owing to high gas pressure values all contributed to the dramatic rise in permeability and porosity observed in concrete at elevated temperatures. The degree to which cracks occur in concrete is another factor in determining its permeability in addition to temperature, moisture, and gas pressure.

Deprivation of the cementitious matrix is the primary cause of the degrading mechanisms of LFC. Although both mechanical and chemical degradation lead to a loss of mechanical characteristics, these two pathways operate at quite different temperatures. Above around 110 °C, dehydration in the cement paste becomes considerable, significantly weakening the C-S-H linkages that are the major creation in hydrated cement paste [28]. Additionally, the limited cement paste permeability property allows inner water pressure to accumulate throughout the dehydration of C-S-H. This raises inner stresses and results in microcracks starting at about 300 °C, which lowers the material's strength and stiffness. The dissociation of calcium hydroxide causes LFC to shrink at temperatures above 450 °C [29]. Calcium oxide in LFC converts into calcium hydroxide when subjected to water at elevated temperatures; this results in cracking and destruction of LFC if the chemical is used in firefighting. It is still very challenging to make reliable predictions about these systems; thus, continued experimentation is necessary [30].

Researchers have been concerned with the fire resistance of LFC for a long time. Kearsley and Mostert [31] looked at how the type of cement affected the performance of LFC at high temperatures. They found that LFC made with hydraulic cement that has an aluminum oxide and calcium oxide ratio can endure high temperatures up to 1500 °C without breaking. A research effort by Sayadi et al. [32] together with Vilches et al. [33] looked at how expanded polystyrene particles affect fire resistance performance. They found that as the volume of expanded polystyrene particles increased, fire resistance reduced dramatically. Jones and McCarthy [34] summed up that LFC of lower densities had better fire resistance than vermiculite concrete. Othuman and Wang [35] proposed two ways to figure out the LFC thermal diffusivity and conductivity values at elevated temperatures. They also came to the conclusion that LFC could be used instead of gypsum to build partition walls. LFC's internal pore structure deteriorating due to elevated temperature exposure is the fundamental internal reason for the depreciation of durability characteristics; hence, studying the change law of these properties is vital to understanding how buildings react in a fire [36]. As the temperature in LFC rises to between 100 °C and 400 °C, the micropore structure cracks, and the porosity increases due to the water evaporation and decarbonization process [37]. Above 400 °C, the major reasons for the subsequent degradation of concrete's pore structure are the dehydration and decomposition of hydration products, which causes a rise in the voids and an expansion in the diameter of voids [38]. Hence, the aim of this investigation was, therefore, to evaluate the LFC mechanical properties through experimental analysis at high temperatures. Varying temperatures, up to 800 °C, were used in the tests. Extensive compressive, flexural, and splitting tensile tests were executed for LFC with densities of 500, 1000, and 1500 kg/m^3.

2. Materials and Mix Design

In this laboratory assessment, LFC was made of cement, sand, water, and surfactant. A cement–sand proportion of 2:1 and a water–cement proportion of 0.5 were employed in order to examine the mechanical properties of LFC exposed to elevated temperatures. The mix proportion for the three densities prepared in this investigation is shown in Table 1. The

mechanical characteristics of LFC cast samples with densities of 500, 1000, and 1500 kg/m^3 were investigated.

Table 1. Mixture proportions of LFC.

Density (kg/m^3)	Cement (kg/m^3)	Sand (kg/m^3)	Water (kg/m^3)	Foam (kg/m^3)
500	327.2	163.6	81.8	46.3
1000	631.6	315.8	157.9	30.7
1500	936.0	468.0	234.0	15.1

All LFC specimens used for testing mechanical properties were produced at the concrete lab. The foam generator Portafoam TM2 System, which was supplied by DRN Technologies, was used to create the stable foam (Figure 1a). This system has a main generator, a foaming unit, and a lancing unit. It is powered by an air compressor. A protein-based foaming agent suitable for LFC densities between 500 kg/m^3 and 1500 kg/m^3 was employed. The cement, fine filler, clean water, and surfactant were mixed until a homogenous mixture was obtained (Figure 1b). For each density, three identical specimens were created and tested 28 days after mixing for compression, flexural and porosity tests.
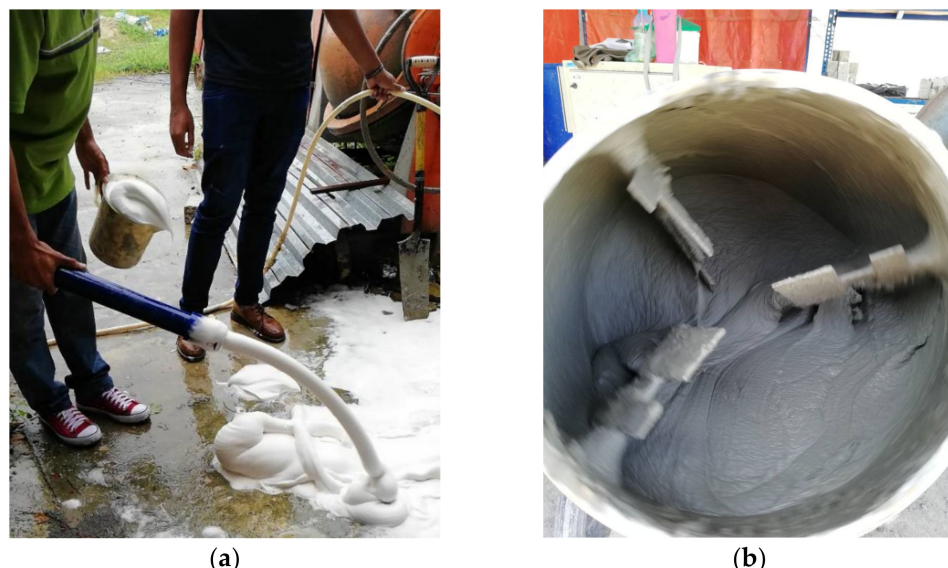

(**a**)   (**b**)

Figure 1. Preparation of LFC mixture. (**a**) stable foam; (**b**) uniform LFC mix.

3. Test Procedure

The unstressed test method was applied in this investigation out of convenience. LFC specimens were heated at a continuous pace without preloading to the predetermined temperature. Up until sample failure, the load was applied at a predetermined pace while keeping the desired temperature. Utilizing an electric furnace (Figure 2), the samples were heated to a range of steady-state temperatures up to 800 °C. A type K thermocouple was placed inside the heating chamber to measure the temperature. Pre-testing tests on the furnaces' power systems and controllers showed that they could maintain the furnaces' operating temperatures within 0.5 °C.

Cylinders measuring 100 × 200 mm underwent compression strength tests. Two strain gauges were attached to each sample to track the behavior of strain under loading at ambient temperature. The strain measurements at normal temperature were employed to verify that the strain computed based on the displacement of the loading plate was precise enough as no strain measurements were made at elevated temperatures. Four Type

K thermocouples were put in the center plane of each LFC sample to measure the LFC cylinder sample temperature, as displayed in Figure 3.
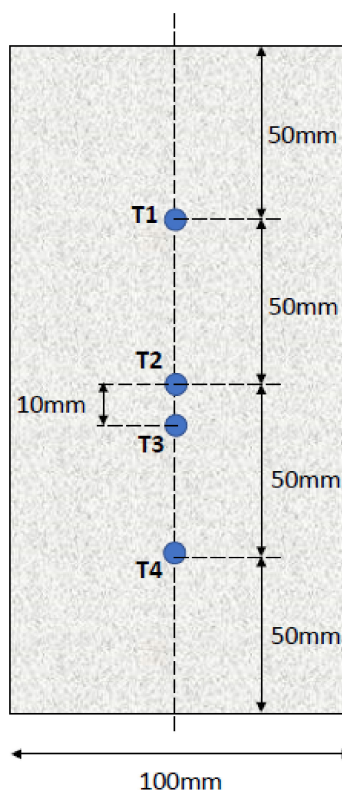

Figure 2. Electric furnace.

Figure 3. Typical LFC cylinder sample with thermocouples arrangement.

After removing the LFC specimens from the furnace, loading was carried out using a compression machine that operated at room temperature. Each specimen was removed from the electric furnace and instantly covered in insulating sheets to prevent heat loss to the atmosphere. To guarantee the consistency of results, three replicate tests were run for each set of tests. Figure 4 shows the setup for the axial compression test.

Figure 4. Setup for axial compression test to determine the compressive strength of LFC.

For ease of use, the bending test was applied in this study. The method for sample preparation was the same as that used for the compression testing previously mentioned. The samples were rectangular parallelepipeds of 125 mm in width, 350 mm in length, and with a height of 25 mm. Simple support and point load at the central point were applied to the LFC specimen. Ls = 200 mm, or the distance between the supports, produced an aspect ratio of Ls/h of 8, which guaranteed that bending behavior would predominate. To calculate the flexural tensile strength, the load–deflection was measured. Figure 5 demonstrates the setup for the three-point bending test.

Figure 5. Setup for three-point bending test to determine the flexural strength of LFC.

Next, the vacuum saturation apparatus was used to ascertain the porosity of LFC. The following equation was used to calculate porosity:

$$\varepsilon = \frac{(W_{sat} - W_{dry})}{(W_{sat} - W_{wat})} \times 100 \tag{1}$$

where ε is the LFC porosity (%), W_{sat} is the LFC specimen weight in the air of the saturated sample, W_{wat} is the LFC sample weight in the water of the saturated specimen, and W_{dry} is the oven-dried LFC specimen weight.

4. Results

4.1. Porosity

The LFC porosity increased as the temperature rose. These variations in porosity values can be explained by examining the phase shifts of LFC at different temperatures. Figure 6 displays the LFC porosity for each density at varying exposing temperatures. The porosity of LFC grew evenly across all three densities. For densities of 500, 1000, and 1500 kg/m^3, the initial porosity was 80.1%, 46.5%, and 22.2%, respectively. Due to the disintegration of C-S-H and sulfoaluminate at 200 °C and 300 °C, the porosity of the higher-density LFC (1000 and 1500 kg/m^3) increased significantly, whereas the increase for the lower-density LFC (500 kg/m^3) was more modest. At 300 °C, the observed porosity for densities of 500, 1000, and 1500 kg/m^3 was 82.2%, 49.8%, and 25.5%, respectively. Due to the disintegration of calcium hydroxide into calcium oxide at temperatures over 400 °C, the observed porosity rose somewhat. At 600 °C, the porosity of 500, 1000 and 1500 kg/m^3 was 83.9%, 52.3%, and 28.5%, respectively. However, owing to its high porosity at room temperature, LFC may be deemed to have a steady porosity across a range of temperatures.
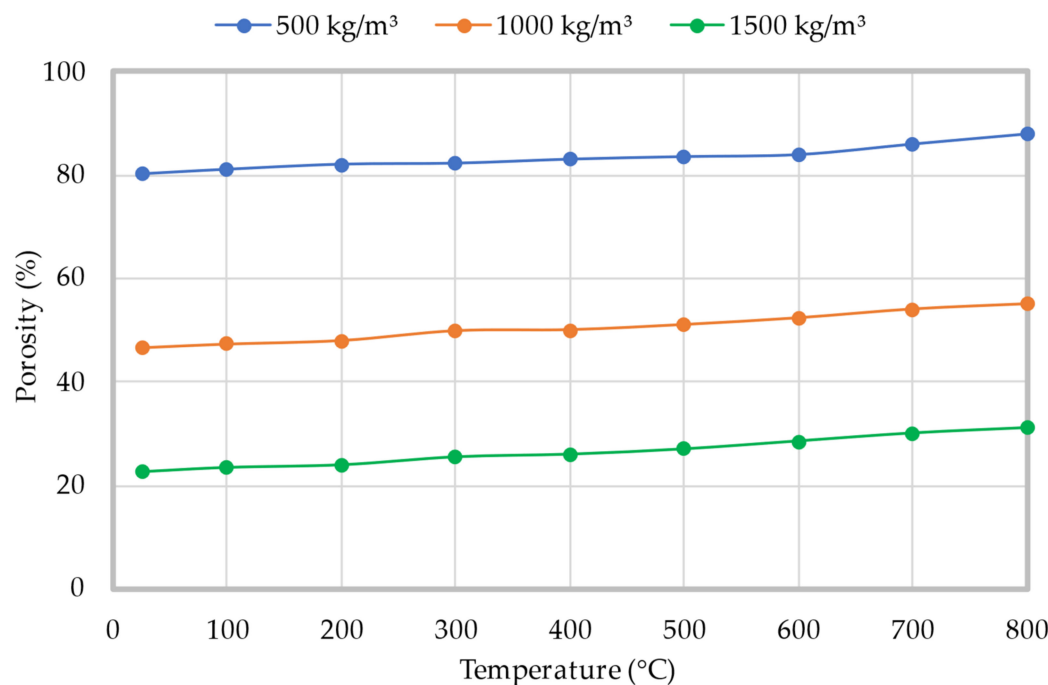

Figure 6. Influence of LFC density on its porosity value at varying temperatures.

Figure 7 displays SEM micrographs of the inner structure of 1500, 1000 and 500 kg/m^3 density LFC at room temperature and at 600 °C, as well as the pore distributions of LFC. Figure 7a–c indicate that void sizes were not consistent and that the typical void size was largely influenced by the LFC density. After exposure to high temperatures, the same SEM analysis was repeated on all three densities, and the SEM findings suggest that the LFC void distribution and size did not change significantly when exposed to 600 °C compared to the specimen at ambient temperature.
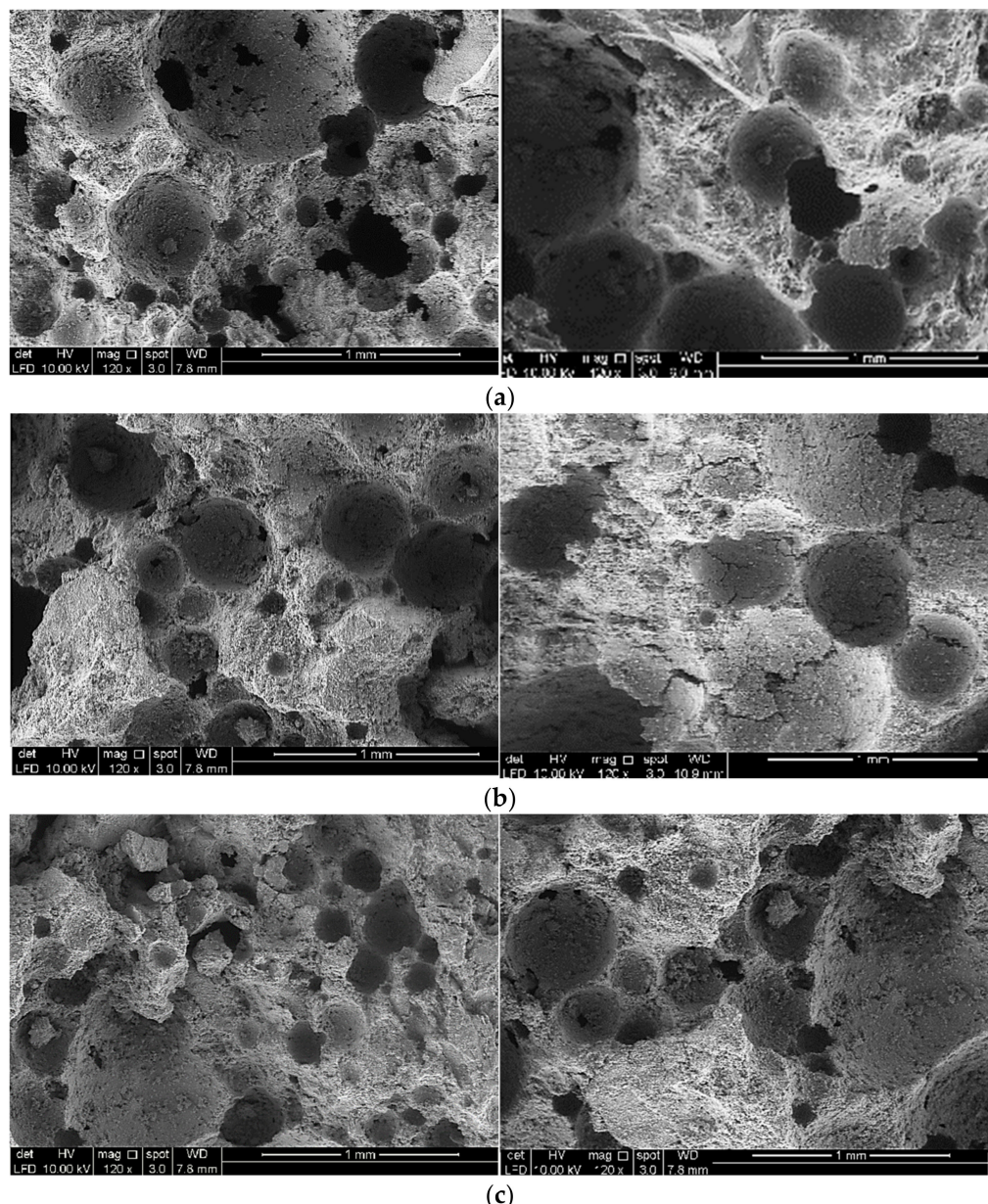
Figure 7. Comparison of SEM micrographs of varying densities at ambient temperature and after exposure to 600 °C. (**a**) 500 kg/m³ density at 20 °C (left) and at 600 °C (right); (**b**) 1000 kg/m³ density at 20 °C (left) and at 600 °C (right); (**c**) 1500 kg/m³ density at 20 °C (left) and at 600 °C (right).

4.2. Compressive Strength

The effect of high temperatures on the LFC compressive strength and normalized strength ratio is depicted in Figures 8 and 9. The normalized compressive strength ratio was calculated by dividing by their respective compressive strength at specific high temperatures from the ambient temperature compressive strength (at 20 °C). These normalized values (%) can be used to compare the rate of decrease in compressive strength at specific high temperatures. According to Figures 8 and 9, the LFC compressive strength decreased with temperature for entire densities considered in this investigation. Upon primary heating, the LFC specimen which was fabricated with OPC got away from the absorbed, evaporable water, followed by the water that was chemically bonded. The loss of water would result in microcracking and a decline in compressive strength. Between 90 °C and 180 °C, the strength under compression dropped gradually due to the discharge of free water and chemically bound water. The drop in compressive strength between

25 °C and 160 °C resembles a decrease in the cohesiveness of Van der Waals forces (a distance-dependent interatomic or molecular interaction) between the layers of C-S-H. This reduces the C-S-H surface energy and results in the production of silanol bands with decreased overall bonding strength.
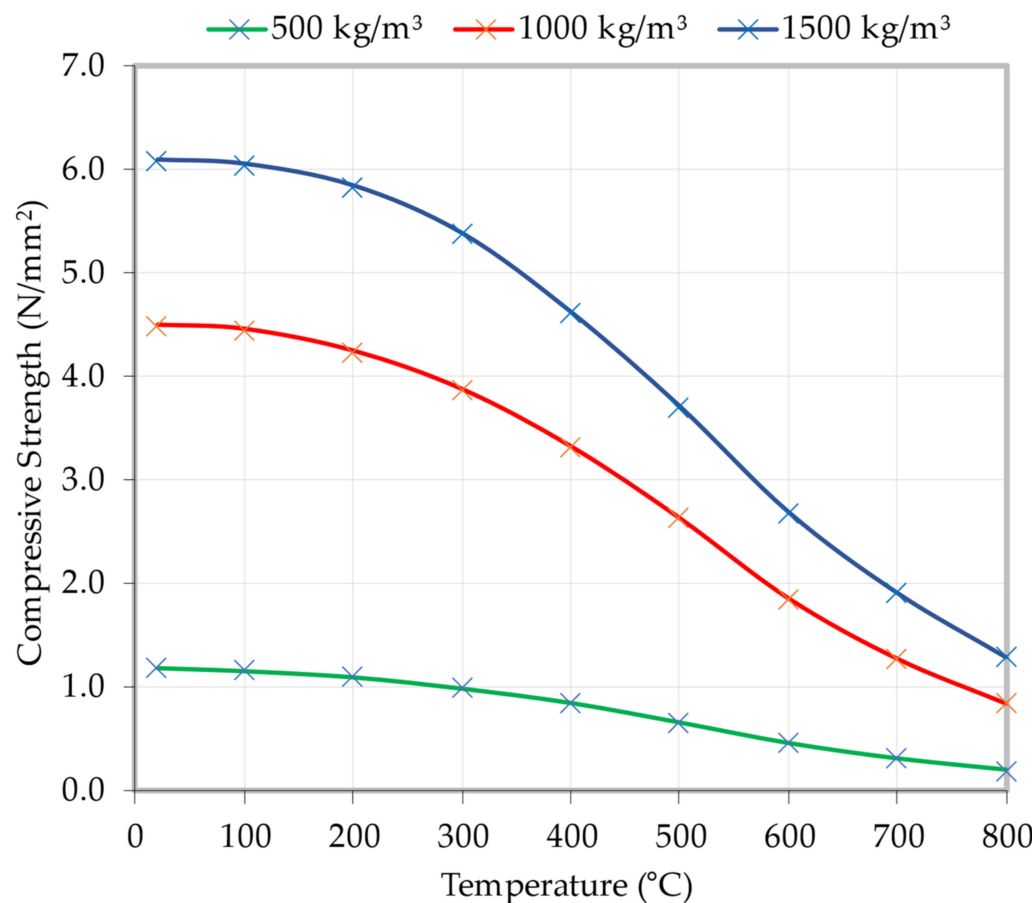

Figure 8. Influence of varying temperatures on the LFC compressive strength.

Nevertheless, because this alteration primarily influenced the LFC surface, the drop in LFC strength was negligible, and the compressive strength specimens at 200 °C remained at approximately 89% of the unheated value. Chang et al. [39] validated this performance by studying concrete compressive strength following high-temperature exposure. According to a comparison of the literature and the current investigation, the decrease in compressive strength under increased temperature (200 °C) was 17%. In this investigation, the compressive strength of all densities of LFC decreased between 5% to 7%. Between 200 °C and 400 °C, the specimens fractured due to the dissolution of sulfoaluminate forms and C-S-H. Significant implications of these cracks on the compressive strength of LFC.

The LFC strength at 400 °C was approximately between 72% and 76% of its starting value for all three densities considered in this study. At high temperatures, deterioration and loss of strength continued to occur. LFC preserved just around 39% to 44% of their initial strength at a temperature of 600 °C. As the proportions of both densities of LFC are comparable, with the exception of more voids in the lower-density LFC, it is not startling that their normalized strength–temperature relations were nearly identical for 500, 1000 and 1500 kg/m³ densities.
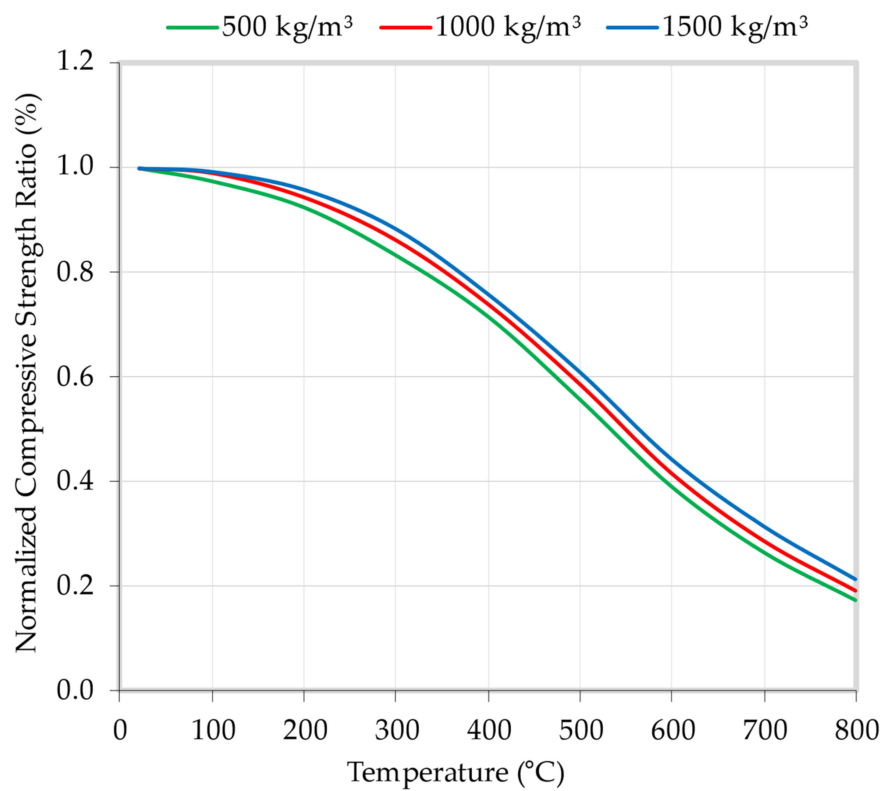
Figure 9. Influence of varying temperatures on the normalized LFC compressive strength.

4.3. Compressive Stress–Strain Correlation

The experiments were regulated for displacement so that the crack persisted to develop and grow after the maximum load was achieved. Due to the brittle breakdown of the test specimens after reaching the highest stress, the downward section of the stress–strain relationship could not be determined. The average stress–strain curves for the three densities at all testing temperatures up to 800 °C are depicted in Figures 10–12. Figures 10–12 demonstrate that for all three densities and temperature ranges, the rising branch was linear for stresses up to 70% of the material's maximum strength for all three densities. At higher temperatures, the strain associated with the maximum strength rose. For LFC with a density of 500 kg/m^3, the highest strains were 0.0035, 0.0040, 0.0050, 0.0057 and 0.0065 at ambient temperature, 200, 400, 600 and 800 °C, whereas for LFC with a density of 1500 kg/m^3, the highest strains were 0.0020, 0.0024, 0.0029, 0.0034 and 0.0039 at room temperature, 200, 400, 600 and 800 °C. The increase in strain was the result of temperatures and heating causing the opening of cracks.

4.4. Young's Modulus in Compression

Figures 13 and 14 depict the temperature-dependent variations in Young's modulus of LFC under compressive load. From the stress–strain curve, Young's modulus was determined as the secant modulus at the spot the LFC material shifted from elastic to plastic form. Greater than the decrease in LFC strength was the decrease in Young's modulus. Both figures demonstrate that the decrease in Young's modulus began as soon as the samples began to dry upon heating. This resulted from the incompatibility of the thermal expansions of LFC cement paste and fine filler at high temperatures [40–42]. Fine sand expands as the temperature rises; however, the C-S-H gel removes both chemically and physically bonded water, resulting in shrinkage and fracture formation. Another effect could be the weakening of cohesive forces brought on by this temperature's water expansion [43,44]. Some silicate aggregates begin to disintegrate as the temperature exceeds about 400 °C, which lowers the strength. At 200, 400, 600 and 800 °C, the modulus of elasticity was approximately 94%, 73%, 40%, and 20% of the original value for all three

densities considered in this study. As with differences in LFC normalized strengths at high temperatures, the normalized Young's modulus of LFC at the same temperature was nearly the same. The Young's modulus in compression went down when the temperature was raised and the LFC specimens lost water and voids.
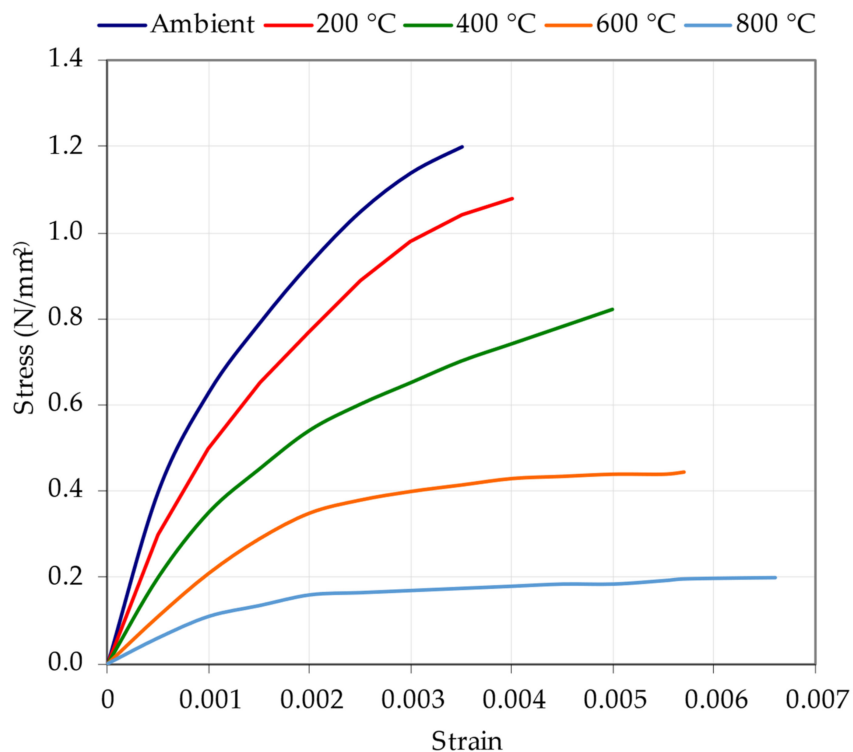

Figure 10. Stress–strain relationship for 500 kg/m^3 density at varying temperatures.
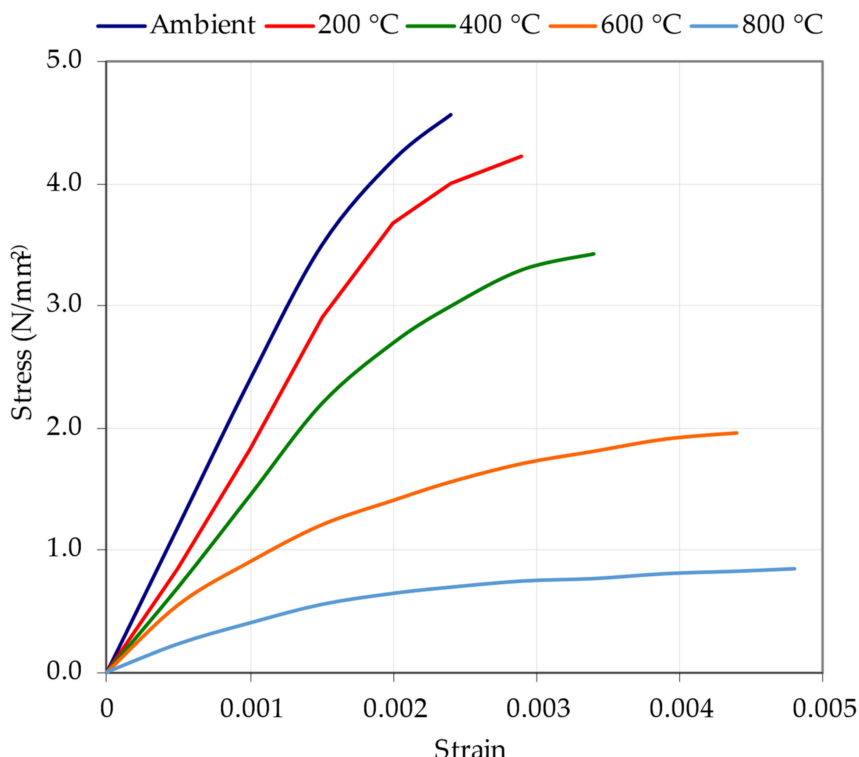

Figure 11. Stress–strain relationship for 1000 kg/m^3 density at varying temperatures.
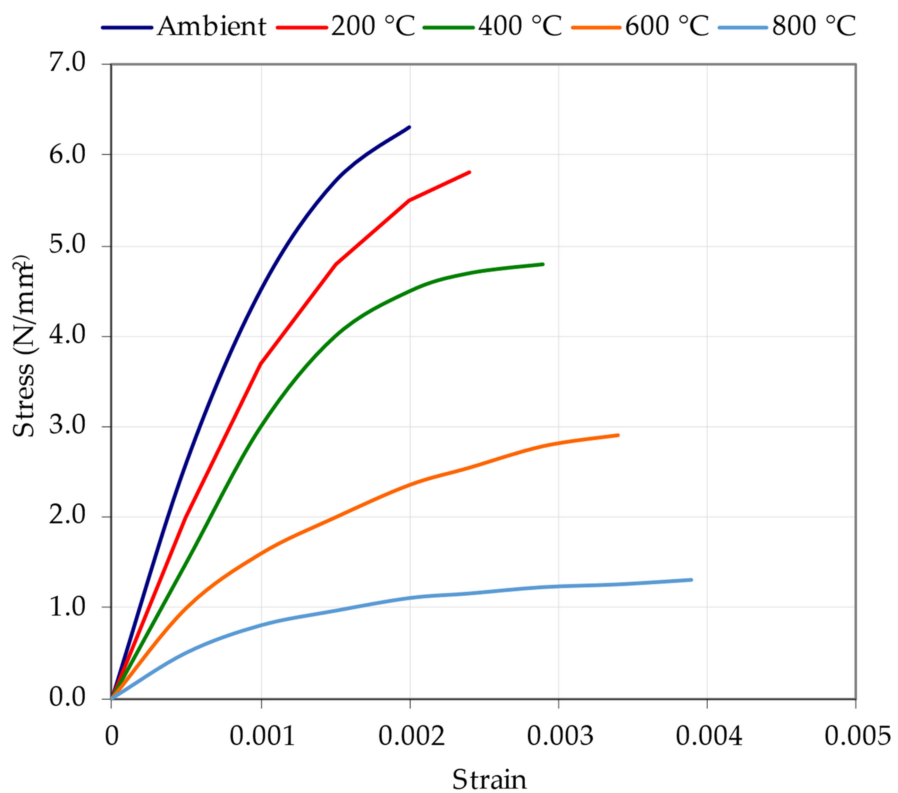
Figure 12. Stress–strain relationship for 1500 kg/m^3 density at varying temperatures.
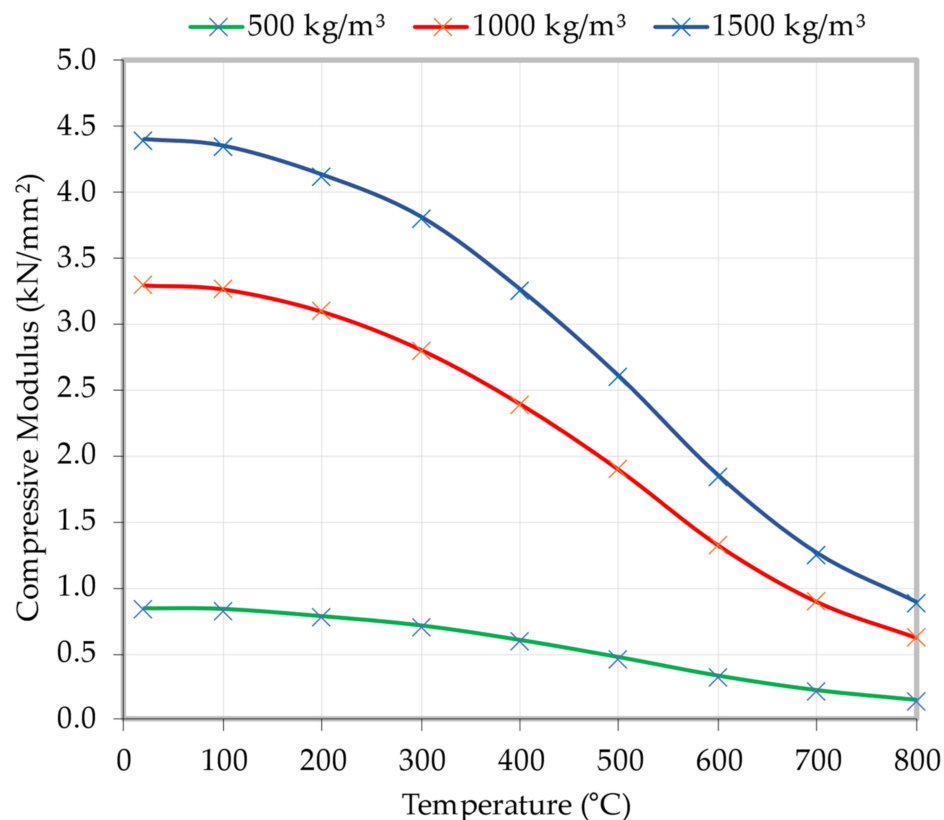

Figure 13. Influence of varying temperatures on the LFC compressive modulus.
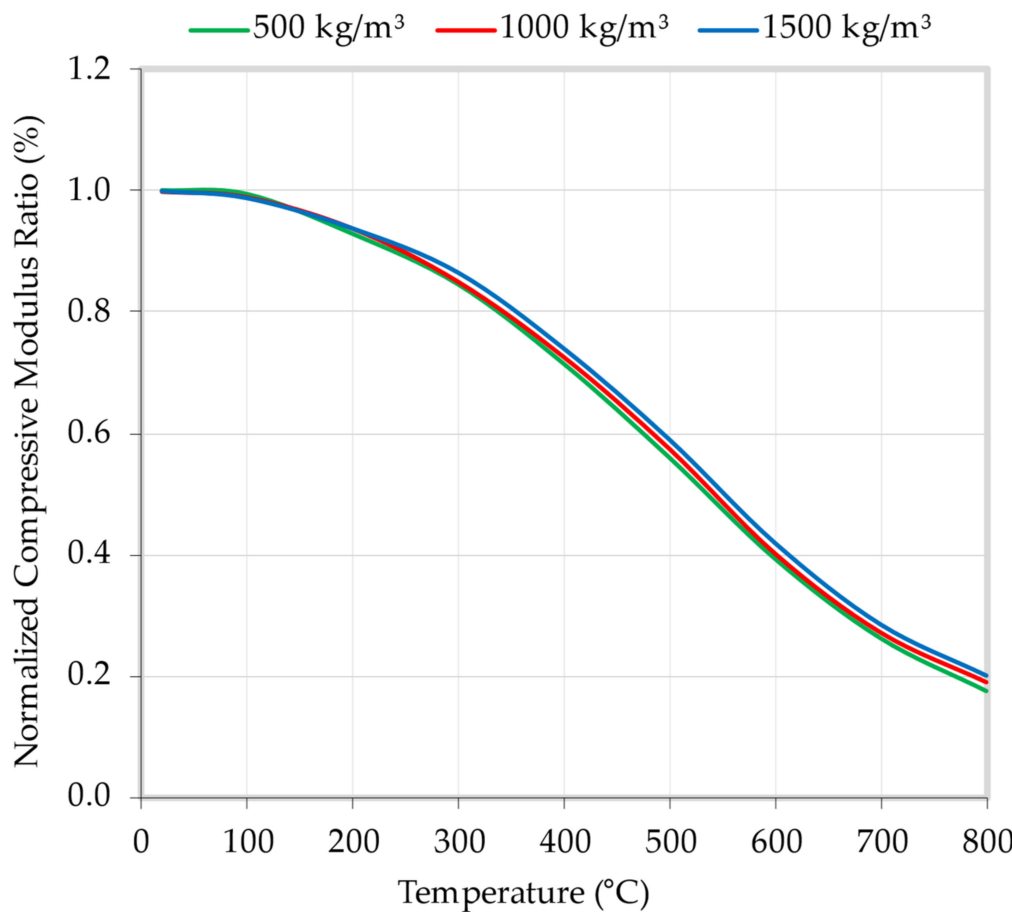
Figure 14. Influence of varying temperatures on the normalized LFC compressive modulus.

4.5. Flexural Strength

The flexural test on the LFC specimen was designed to gauge the bending strength of LFC. Figures 15 and 16 show the temperature-dependent change in the flexural tensile strength of LFC. Above 100 °C, LFC's flexural tensile strength started to drop markedly regardless of density. Microcracking, which appears as free and chemically bonded water vaporizes, is the primary process driving the degradation of LFC, and this is in line with variations in the other mechanical properties. Cracks appeared and tensile strength drastically dropped when the chemical structure of LFC began to degrade between 200 °C and 300 °C as a result of the dissolution of the sulfoaluminate phases. All densities saw a reduction in tensile strength to roughly 58% to 63% at 400 °C. Flexural tensile strength was only 20% at 800 °C for densities of 500, 1000 and 1500 kg/m^3. The production of spreading fractures accounted for the rapid fall in flexural strength from 400 °C to 800 °C. The binding between LFC fine filler and the cementitious matrix was reduced by internal shrinkage due to the evaporation of free water as well as the chemically bound water. When subjected to the same thermal treatment, flexural strength suffered more than compressive strength.
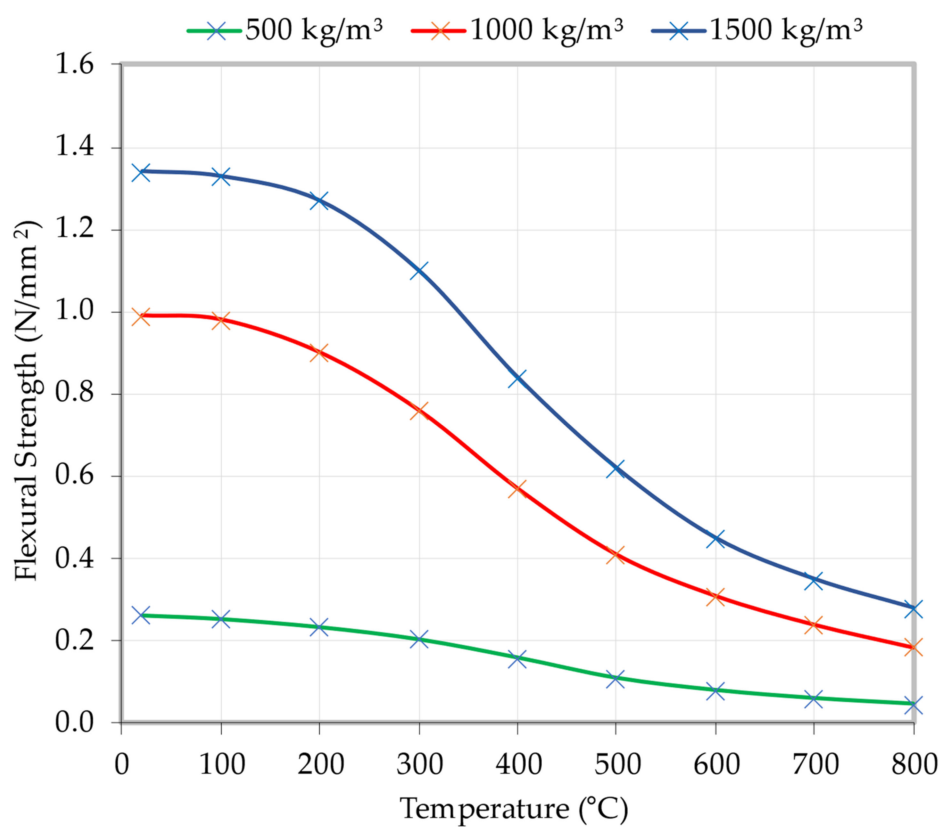
Figure 15. Influence of varying temperatures on the LFC flexural strength.
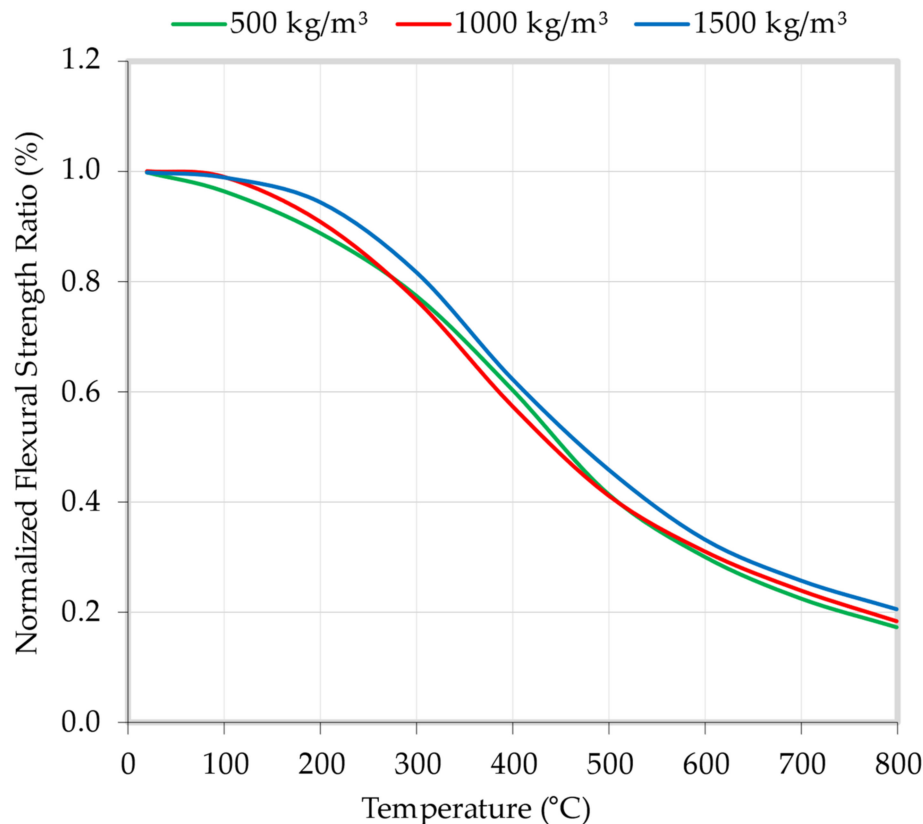

Figure 16. Influence of varying temperatures on the normalized LFC flexural strength.

5. Conclusions

This study presents the results of a series of experiments designed to measure the compressive and tensile mechanical properties of LFC at elevated temperatures. Different densities of LFC were tested in compression cylinders and in three-point bending at temperatures ranging from room temperature to 800 °C. Mechanical properties such as compressive strength, compressive Young's modulus, compressive stress–strain relationship, porosity, and flexural strength were evaluated. Regardless of density, the testing results showed that at high temperatures, LFC lost most of its stiffness after about 100 °C. This hints at the fact that microcracking is the primary process causing stiffness loss, as it develops as the water grows and dissolves. It stands to reason that LFC's strength and stiffness would change when its density was increased. LFC of varying densities poses interestingly similar normalized strength and stiffness–temperature relations.

Institutional Review Board Statement: Not applicable.

Informed Consent Statement: Not applicable.

Data Availability Statement: Not applicable.

Conflicts of Interest: The author declares no conflict of interest.

References

1. Lin, Y.S. Estimations of the probability of fire occurrences in buildings. *Fire Saf. J.* **2005**, *40*, 728–735. [CrossRef]
2. Joint ACI/TMS Committee 216 and Masonry Society (U.S.). *Code Requirements for Determining Fire Resistance of Concrete and Masonry Construction Assemblies (ACI 216.1-14, TMS-216-14): An ACI/TMS Standard*; American Concrete Institute: Farmington Hills, MI, USA, 2014.
3. Tan, X.; Chen, W.; Wang, J.; Yang, D.; Qi, X.; Ma, Y.; Wang, X.; Ma, S.; Li, C. Influence of high temperature on the residual physical and mechanical properties of foamed concrete. *Constr. Build. Mater.* **2017**, *135*, 203–211. [CrossRef]
4. Othuman, M.A.; Wang, Y.C. Elevated-temperature thermal properties of lightweight foamed concrete. *Constr. Build. Mater.* **2011**, *25*, 705–716. [CrossRef]
5. Richard, A.O.; Ramli, M. Experimental production of sustainable lightweight foamed concrete. *Br. J. Appl. Sci. Technol.* **2013**, *3*, 994. [CrossRef]
6. Choumanidis, D.; Badogiannis, E.; Nomikos, P.; Sofianos, A. The effect of different fibres on the flexural behaviour of concrete exposed to normal and elevated temperatures. *Constr. Build. Mater.* **2016**, *129*, 266–277. [CrossRef]
7. Mehrabi, P.; Shariati, M.; Kabirifar, K.; Jarrah, M.; Rasekh, H.; Trung, N.T.; Shariati, A.; Jahandari, S. Effect of pumice powder and nano-clay on the strength and permeability of fiber-reinforced pervious concrete incorporating recycled concrete aggregate. *Constr. Build. Mater.* **2021**, *287*, 122652. [CrossRef]
8. Toghroli, A.; Mehrabi, P.; Shariati, M.; Trung, N.T.; Jahandari, S.; Rasekh, H. Evaluating the use of recycled concrete aggregate and pozzolanic additives in fiber-reinforced pervious concrete with industrial and recycled fibers. *Constr. Build. Mater.* **2021**, *252*, 118997. [CrossRef]
9. Agra, R.R.; Serafini, R.; de Figueiredo, A.D. Effect of high temperature on the mechanical properties of concrete reinforced with different fiber contents. *Constr. Build. Mater.* **2021**, *301*, 124242. [CrossRef]
10. Lee, T.; Kim, G.; Choe, G.; Hwang, E.; Lee, J.; Ryu, D.; Nam, J. Spalling Resistance of Fiber-Reinforced Ultra-High-Strength Concrete Subjected to the ISO-834 Standard Fire Curve: Effects of Thermal Strain and Water Vapor Pressure. *Materials* **2020**, *13*, 3792. [CrossRef]
11. *EN 1992-1-2*; Eurocode 2: Design of Concrete Structures-Part 1–2: General Rules-Structural Fire Design. The European Union: Mestreech, The Netherlands, 1992.
12. Nasser, I.M.; Ibrahim, M.H.W.; Zuki, S.S.M.; Algaif, H.A.; Alshalif, A.F. The effect of nanosilica incorporation on the mechanical properties of concrete exposed to elevated temperature: A review. *Environ. Sci. Pollut. Res.* **2022**, *29*, 15318–15336. [CrossRef]
13. Sharifianjazi, F.; Zeydi, P.; Bazli, M.; Esmaeilkhanian, A.; Rahmani, R.; Bazli, L.; Khaksar, S. Fibre-Reinforced Polymer Reinforced Concrete Members under Elevated Temperatures: A Review on Structural Performance. *Polymers* **2022**, *14*, 472. [CrossRef]
14. Anderberg, G.A.; Both, Y.; Fellinger, K.; Høj, J.; Khoury, N.P.M.C. *Fire Design of Concrete Structures-Materials, Structures and Modelling*; Fib Bulletin 46; International Federation for Structural Concrete: Lausanne, Swizerland, 2007.

15.   Mydin, M.A.O.; Phius, A.F.; Sani NMd Tawil, N.M. Potential of Green Construction in Malaysia: Industrialised Building System (IBS) vs Traditional Construction Method. *E3S Web Conf.* **2014**, *3*, 01009. [CrossRef]

16.   Mohamad, N.; Iman, M.A.; Othuman Mydin, M.A.; Samad, A.A.A.; Rosli, J.A.; Noorwirdawati, A. Mechanical properties and flexure behaviour of lightweight foamed concrete incorporating coir fibre. *IOP Conference Series: Earth Environ. Sci.* **2018**, *140*, 012140. [CrossRef]

17.   Serri, E.; Suleiman, M.Z.; Mydin, M.A.O. The effects of oil palm shell aggregate shape on the thermal properties and density of concrete. *Adv. Mat. Res.* **2014**, *935*, 172–175.

18.   Mohamad, N.; Samad, A.A.A.; Lakhiar, M.T.; Othuman Mydin, M.A.; Jusoh, S.; Sofia, A.; Efendi, S.A. Effects of Incorporating Banana Skin Powder (BSP) and Palm Oil Fuel Ash (POFA) on Mechanical Properties of Lightweight Foamed Concrete. *Int. J. Int. Eng.* **2018**, *10*, 69–76. [CrossRef]

19.   Ganesan, S.; Othuman Mydin, M.A.; Sani, N.M.; Che Ani, A.I. Performance of polymer modified mortar with different dosage of polymeric modifier. *MATEC Web Conf.* **2014**, *15*, 01039. [CrossRef]

20.   Nambiar, E.K.K.; Ramamurthy, K. Air-void characterisation of foam concrete. *Cem. Concr. Res.* **2007**, *37*, 221–230. [CrossRef]

21.   Othuman Mydin, M.A.; Mohamed Shajahan, M.F.; Ganesan, S.; Sani, N.M. Laboratory investigation on compressive strength and micro-structural features of foamed concrete with addition of wood ash and silica fume as a cement replacement. *MATEC Web Conf.* **2014**, *17*, 01004. [CrossRef]

22.   Tambichik, M.A.; Abdul Samad, A.A.; Mohamad, N.; Mohd Ali, A.Z.; Othuman Mydin, M.A.; Mohd Bosro, M.Z.; Iman, M.A. Effect of combining Palm Oil Fuel Ash (POFA) and Rice Husk Ash (RHA) as partial cement replacement to the compressive strength of concrete. *Int. J. Integr. Eng.* **2018**, *10*, 61–67. [CrossRef]

23.   Dhasindrakrishna, K.; Ramakrishnan, S.; Pasupathy, K.; Sanjayan, J. Collapse of fresh foam concrete: Mechanisms and influencing parameters. *Cem. Concr. Compos.* **2021**, *122*, 104151. [CrossRef]

24.   Falliano, D.; Parmigiani, S.; Suarez-Riera, D.; Ferro, G.A.; Restuccia, L. Stability, flexural behavior and compressive strength of ultra-lightweight fiber-reinforced foamed concrete with dry density lower than 100 kg/m3. *J. Build. Eng.* **2022**, *51*, 104329. [CrossRef]

25.   Awang, H.; Mydin, M.A.O.; Roslan, A.F. Effects of fibre on drying shrinkage, compressive and flexural strength of lightweight foamed concrete. *Adv. Mat. Res.* **2012**, *587*, 144–149.

26.   Lin, W.M.; Lina, T.D.; Powers-Couche, L.J. Microstructures of fire-damaged concrete. *J. Am. Concr. Inst. Mater.* **1996**, *93*, 199–205.

27.   Li, Y.; Yang, E.-H.; Tan, K.H. Flexural behavior of ultra-high performance hybrid fiber reinforced concrete at the ambient and elevated temperature. *Constr. Build. Mater.* **2020**, *250*, 118487. [CrossRef]

28.   Serafini, R.; Dantas, S.R.; Salvador, R.P.; Agra, R.R.; Rambo, D.A.; Berto, A.F.; de Figueiredo, A.D. Influence of fire on temperature gradient and physical-mechanical properties of macro-synthetic fiber reinforced concrete for tunnel linings. *Constr. Build. Mater.* **2019**, *214*, 254–268. [CrossRef]

29.   Hua, N.; Khorasani, N.E.; Tessari, A.; Ranade, R. Experimental study of fire damage to reinforced concrete tunnel slabs. *Fire Saf. J.* **2022**, *127*, 103504. [CrossRef]

30.   Serafini, R.; de La Fuente, A.; de Figueiredo, A.D. Assessment of the post-fire residual bearing capacity of FRC and hybrid RC-FRC tunnel sections considering thermal spalling. *Mater. Struct.* **2021**, *54*, 219. [CrossRef]

31.   Kearsley, E.P.; Mostert, H.F. The use of foamed concrete in refractories. In *Use of Foamed Concrete in Construction*; Thomas Telford: London, UK, 2005; pp. 89–96.

32.   Sayadi, A.A.; Tapia, J.V.; Neitzert, T.R.; Clifton, G.C. Effects of expanded polystyrene (EPS) particles on fire resistance, thermal conductivity and compressive strength of foamed concrete. *Constr. Build. Mater.* **2016**, *112*, 716–724. [CrossRef]

33.   Vilches, J.; Ramezani, M.; Neitzert, T. Experimental investigation of the fire resistance of ultra lightweight foamed concrete. *Int. J. Adv. Eng. Appl.* **2012**, *1*, 15–22.

34.   Jones, M.R.; McCarthy, A. Preliminary views on the potential of foamed concrete as a structural material. *Mag. Concr. Res.* **2015**, *57*, 21–32. [CrossRef]

35.   Othuman Mydin, M.A.; Zamzani, N.M.; Ghani, A.N.A. Experimental data on compressive and flexural strengths of coir fibre reinforced foamed concrete at elevated temperatures. *Data in Brief.* **2019**, *25*, 104230. [CrossRef]

36.   Bingöl, A.F.; Gül, R. Effect of elevated temperatures and cooling regimes on normal strength concrete. *Fire Mater.* **2008**, *33*, 79–88. [CrossRef]

37.   Botte, W.; Caspeele, R. Post-cooling properties of concrete exposed to fire. *Fire Saf. J.* **2017**, *92*, 142–150. [CrossRef]

38.   Carette, G.G.; Painter, K.E.; Malhotra, V.M. Sustained high temperature effects on concrete made with normal Portland cement, normal Portland cement and slag, or normal Portland cement and fly ash. *Concr. Int.* **1982**, *4*, 41–51.

39.   Chang, Y.F.; Chen, Y.H.; Sheu, M.S.; Yao, G.C. Residual stress–strain relationship for concrete after exposure to high temperatures. *Cem. Concr. Res.* **2006**, *36*, 1999–2005. [CrossRef]

40.   Yüksel, I.; Siddique, R.; Ozkan, O. Influence of high temperature on the properties of concretes made with industrial by-products as fine aggregate replacement. *Constr. Build. Mater.* **2011**, *25*, 967–972. [CrossRef]

41.   Poon, C.S.; Azhar, S.; Anson, M.; Wong, Y.-L. Comparison of the strength and durability performance of normal- and high-strength pozzolanic concretes at elevated temperatures. *Cem. Concr. Res.* **2001**, *31*, 1291–1300. [CrossRef]

42. Siddique, R.; Kaur, D. Properties of concrete containing ground granulated blast furnace slag (GGBFS) at elevated temperatures. *J. Adv. Res.* **2011**, *3*, 45–51. [CrossRef]
43. Peng, G.-F.; Bian, S.-H.; Guo, Z.-Q.; Zhao, J.; Peng, X.-L.; Jiang, Y.-C. Effect of thermal shock due to rapid cooling on residual mechanical properties of fiber concrete exposed to high temperatures. *Constr. Build. Mater.* **2008**, *22*, 948–955. [CrossRef]
44. Yuzer, N.; AkOz, F.; Ozturk, L. Compressive strength–color change relation in mortars at high temperature. *Cem. Concr. Res.* **2004**, *34*, 1803–1807.